

Article

Mechanical and Impact Properties of Engineered Cementitious Composites Reinforced with PP Fibers at Elevated Temperatures

Raad A. Al-Ameri ¹, Sallal Rashid Abid ^{2,*}  and Mustafa Özakça ¹

¹ Department of Civil Engineering, Gaziantep University, Gaziantep 27310, Turkey; raada.alameri@gmail.com (R.A.A.-A.); ozakca@gantep.edu.tr (M.Ö.)

² Department of Civil Engineering, Wasit University, Kut 52003, Iraq

* Correspondence: sallal@uowasit.edu.iq

Abstract: The repeated impact performance of engineered cementitious composites (ECCs) is not well explored yet, especially after exposure to severe conditions, such as accidental fires. An experimental study was conducted to evaluate the degradation of strength and repeated impact capacity of ECCs reinforced with Polypropylene fibers after high temperature exposure. Compressive strength and flexural strength were tested using cube and beam specimens, while disk specimens were used to conduct repeated impact tests according to the ACI 544-2R procedure. Reference specimens were tested at room temperature, while three other groups were tested after heating to 200 °C, 400 °C and 600 °C and naturally cooled to room temperature. The test results indicated that the reference ECC specimens exhibited a much higher failure impact resistance compared to normal concrete specimens, which was associated with a ductile failure showing a central surface fracture zone and fine surface multi-cracking under repeated impacts. This behavior was also recorded for specimens subjected to 200 °C, while the exposure to 400 °C and 600 °C significantly deteriorated the impact resistance and ductility of ECCs. The recorded failure impact numbers decreased from 259 before heating to 257, 24 and 10 after exposure to 200 °C, 400 °C and 600 °C, respectively. However, after exposure to all temperature levels, the failure impact records of ECCs kept at least four times higher than their corresponding normal concrete ones.

Keywords: repeated impact; ACI 544-2R; high temperatures; fire; ECC; impact ductility



Citation: Al-Ameri, R.A.; Abid, S.R.; Özakça, M. Mechanical and Impact Properties of Engineered Cementitious Composites Reinforced with PP Fibers at Elevated Temperatures. *Fire* **2022**, *5*, 3. <https://doi.org/10.3390/fire5010003>

Academic Editor: Maged A. Youssef

Received: 28 November 2021

Accepted: 26 December 2021

Published: 30 December 2021

Publisher's Note: MDPI stays neutral with regard to jurisdictional claims in published maps and institutional affiliations.



Copyright: © 2021 by the authors. Licensee MDPI, Basel, Switzerland. This article is an open access article distributed under the terms and conditions of the Creative Commons Attribution (CC BY) license (<https://creativecommons.org/licenses/by/4.0/>).

1. Introduction

Regardless of the function and type of occupation of any structural facility, it is still probable to be subjected to unfavorable extreme or accidental loads. Most of the modern reinforced concrete structures are designed to withstand the usual design gravity loads in addition to lateral loads, such as wind and seismic loads. However, considering the accidental loading cases in design is not a typical procedure required by building design codes because this action would distend the construction cost. Among the most probable types of accidental loads are fires and impact loads. The rapid increase of temperature due to the combustion of furniture, nonstructural materials and electrical wiring can noticeably degrade the structural capacity of slabs, beams and columns. On the other hand, sudden impact loads can cause serious concentrated damage that may affect the integrity of the structure.

Although there are great advantages in fire resisting systems and materials in the construction industry, fires keep occurring every day. Large numbers of fire accidents are reported every year [1], where approximately half a million accidental fires were reported between 2013 and 2014 in the USA, while more than 150,000 fire accidents were reported in the UK during the same period. From these fires, 40% were recognized as structural fires [1,2]. Between 1993 and 2016, approximately 90 million fire accidents were recorded

in 39 countries with more than a million death incidences [2]. The crucial question after each structural fire is whether the concrete structure can continue to be occupied as usual, should be rehabilitated before reoccupied or must be demolished [3]. Such a decision needs an accurate estimation of the residual properties of concrete, especially the mechanical strength to withstand the design loads. The physical and chemical actions that take place within the microstructure of concrete depend mainly on the temperature level reached and the fire exposure duration. Yet, the composition of the mixture, its porosity and the thermal properties of aggregate are also leading factors that determine the thermal resistance of concrete structures [3–6]. With the increase of temperature, several chemical and physical changes take place and affect the concrete strength owing to its heterogeneous state [7]. The first physical action of fire occurs at approximately 80 °C to 120 °C, where the contained free water in the concrete evaporates [7–9]. This action has a minor effect on concrete degradation, while the following action that usually occurs at temperatures higher than 300 °C and lower than 450 °C represents the starting point of the serious material degradation. This action is the dehydration of the C-S-H gel from the hydrated cement matrix [9–12]. The following actions depend not only on cement but also on the aggregate type [13–16]. The differences in thermal actions between the cement matrix and aggregate, due to the different thermal properties, result in breaking the bond at higher temperatures, which further weakens the concrete structure and deteriorates its residual strength [7,9]. Previous researchers showed that the tensile strength of concrete deteriorates at a faster rate compared to compressive strength [17,18]. Similarly, mechanical properties such as flexural strength, shear strength and modulus of elasticity showed significant deteriorations after exposure to 500 °C [19–23].

On the other hand, some parts of some structures are frequently subjected to the impact of falling objects or the lateral collision of moving vehicles, which are types of repeated accidental impact loads [24]. Other examples of repeated impacts are the offshore structures, where the waves of ocean water repeatedly subject these structures to hydraulic impacts. In hydraulic structures, such as stilling basins, the water acts as an impacting force on the downstream runway. Other examples of repeated impacts can be the forces subjected by airplane wheels on the airport runways [25–27]. The impact strength of concrete can be investigated using several techniques. However, the repeated impact test introduced by ACI 544-2R “Measurement of Properties of Fiber Reinforced Concrete” [28] is the simplest impact test and the only one that simulates the repeated impact case.

In recent years, several significant studies were conducted to evaluate the repeated impact strength of different concrete types using this testing technique. Mastali et al. [29] investigated the effect of the length and dosage of recycled carbon fiber reinforced polymer on the repeated impact performance of Self-Compacting Concrete (SCC). Ismail and Hassan [30] conducted experimental tests using the ACI 544-2R procedure to evaluate the impact resistance of SCC mixtures that include different contents of Steel Fibers (SF) and crumb rubber. The test results showed that the impact numbers increased by up to 30% and the impact ductility enhanced when crumb rubber was utilized, while the incorporation of 1% of SF significantly improved the retained impact numbers by more than 400%. The mono and dual effects of hooked-end and crimped SF on the ACI 544-2R impact resistance of SCC were investigated by Mahakavi and Chithra [31], where significant impact resistance improvement was reported when the two fiber types were hybridized. Jabir et al. [32] investigated the influence of single and hybrid micro SF and Polypropylene (PP) fibers on the impact resistance of ultra-high performance concrete. Abid et al. conducted ACI 544-2R [33] and flexural [34] repeated impact tests on SCC with micro SF contents of 0.5%, 0.75% and 1.0%. The results indicated that 1.0% of SF could increase the impact resistance by more than 800% compared to the reference plain specimens, while in another study [35], a percentage increase of approximately 1200% was recorded. Murali et al. [36–40] and others [41–43] conducted a series of experimental works that explored the repeated impact capabilities of multi-layered fibrous concrete. Double and triple layered concrete with preplaced aggregate and fibers with grouted cement paste were tested using

the ACI 544-2R. Works on this material [36,37,41] showed that using intermediate fibrous meshes can improve the impact resistance at cracking and failure stages. However, the most influential contribution to impact strength development was attributed to the steel fibers.

Compared to conventional concrete that have similar strength and fiber content, Engineered Cementitious Composites (ECCs) are a type of high-performance SCC concrete that possess extraordinary ductility with strain hardening and multiple cracking under tensile and flexural stresses. ECCs were first introduced by Li in 1993 [44] and used in several applications [45]. Since that time, numerous studies have been conducted to introduce different ECC mixtures with different fiber types and contents. Plenty of research is available in literature on the different mechanical properties of ECCs. However, research on ECC repeated impact behavior is rare. The performance of ECCs under repeated impact was experimentally investigated by Ismail et al. [46] using the ACI 544-2R technique. Different ECC mixtures were introduced using fixed contents of binder, water, sand and fiber. The results indicated that using 15% to 20% metakaolin with fly ash significantly enhanced the impact performance. Similarly, some studies that evaluate the performance and residual mechanical properties of different ECC mixtures after fire exposure are available in literature [47–50].

It is obvious from the introduced literature that very rare experimental works are available in literature on the repeated impact strength of ECCs. Similarly, there is a serious gap of knowledge about the residual impact strength of fibrous concrete after fire temperatures. To the best of the authors' knowledge, no previous research was conducted to study the residual repeated impact strength of ECCs after high temperature exposure. To fill this gap of knowledge, an experimental program was directed in this research to investigate the cracking and failure repeated impact performances and impact ductility of PP-based ECCs after exposure to high temperatures reaching 600 °C. Such type of research is required because both accidental fire and impact loading are expected along the lifespan of structures. Hence, the research outputs can be utilized to evaluate the residual material and structural response of structural members made of ECCs under such accidental cases.

2. Materials and Methods

2.1. Mixtures and Materials

The aim of this study is to evaluate the residual repeated impact performance of ECCs after exposure to elevated temperatures, which can be considered as a type of new concrete that includes no aggregate particles and a high content of fine cementitious and filler materials. The M45 is a typical ECC mixture introduced by leading researchers, which was the base and most widely used mixture with proven characteristics [44,45]. This mixture was used in this study but with PP fiber instead of the typical and much more expensive polyvinyl alcohol fiber (PVA). On the other hand, a normal strength conventional concrete mixture (NC) with an approximately comparative compressive strength was used for comparison purposes. The mix design proportions of both mixtures are detailed in Table 1.

Table 1. Material contents in the ECC and NC mixtures (kg/m³).

Mixture	Cement	Fly Ash	Sand	Silica Sand	Gravel	Water	SP	Fiber
NC	410	NA	787	NA	848	215	NA	NA
ECC	570	684	NA	455	NA	330	4.9	18.2 (2% PP)

A single type of Portland cement (Type 42.5) was used for both mixtures, while fly ash was used as a second cementitious material in the ECC mixture. The chemical composition and physical properties for both cement and fly ash are listed in Table 2. As preceded, the ECC mixture included no sand or gravel, where the filler of the mixture was composed of a single type of very fine silica sand with a grain size of 80 to 250 micrometer and a bulk density of 1500 kg/m³. On the other hand, local sand and crushed gravel from the central

region of Iraq were used as fine and coarse aggregates for the NC mixture. The grading of the sand and gravel are shown in Table 3, while the maximum size of the gravel particles was 10 mm. For the ECC mixture, a super plasticizer (SP) type ViscoCrete 5930-L from Sika® was used to assure the required workability due to the large amount of fine materials, while 2% by volume of PP fiber was used with the properties shown in Table 4.

Table 2. Properties of cement and fly ash.

Oxide (%)	Cement	Fly Ash
SiO ₂	20.08	56.0
Fe ₂ O ₃	3.6	24.81
Al ₂ O ₃	4.62	5.3
CaO	61.61	4.8
MgO	2.12	1.48
SO ₃	2.71	0.36
Loss on ignition (%)	1.38	5.78
Specific surface (m ² /kg)	368	-
Specific gravity	3.15	2.20
Fineness (% retain in 45 µm)	-	28.99

Table 3. Grading of sand and gravel used for NC specimens.

Sieve Size (mm)	Sand % Passing	Gravel % Passing
19	100	100
12.5	100	100
10	100	95.1
4.75	90.7	33.5
2.36	77.9	1.1
1.18	53.5	0
0.6	28.7	0
0.3	7.5	0
0.15	0	0

Table 4. Properties of polypropylene fiber.

Property	Density	Length	Diameter	Tensile Strength	Elastic Modulus
Value	910 kg/m ³	12 mm	0.032 mm	400 MPa	4000 MPa

2.2. Test Program and Heating Regime

From each mixture and for each temperature level, six 150 mm diameter and 64 mm thick disk specimens were used to evaluate the repeated impact test under the free drop-weight procedure of ACI 544-2R. On the other hand, six 100 mm cube specimens were used for a compressive strength test according to BS EN 12390-3: 2009 [51], while six beam specimens with 100 × 100 mm cross section and 400 mm length were tested under four-point bending test (300 mm span) for flexural strength according to BS EN 12390-5: 2009 [52]. All of the disk, cube and beam specimens were cured under the same standard conditions in temperature-controlled water tanks for 28 days.

After the curing period, the specimens were dried in the laboratory environment for 24 h. Previous researchers and trial tests conducted in this study showed that the heating of specimens without initial drying may lead to the explosive failure of some specimens at high temperatures. Therefore, all specimens were pre-dried using an electrical oven at a temperature of approximately 105 °C for 24 h. Afterwards, the specimens were heated using the electrical furnace shown in Figure 1a at a constant rate of approximately 4 °C/min to three levels of high temperatures of 200 °C, 400 °C and 600 °C. When the specified temperature level was reached, the temperature was kept constant for 60 min to assure the thermal saturation at this temperature. Finally, the furnace door was opened

and the specimens were left to cool slowly at the laboratory temperature until testing time. The heating regime of the three temperature levels is described in Figure 1b. In addition to the three groups of heated specimens, a fourth group was tested at room temperature without heating as a reference group.

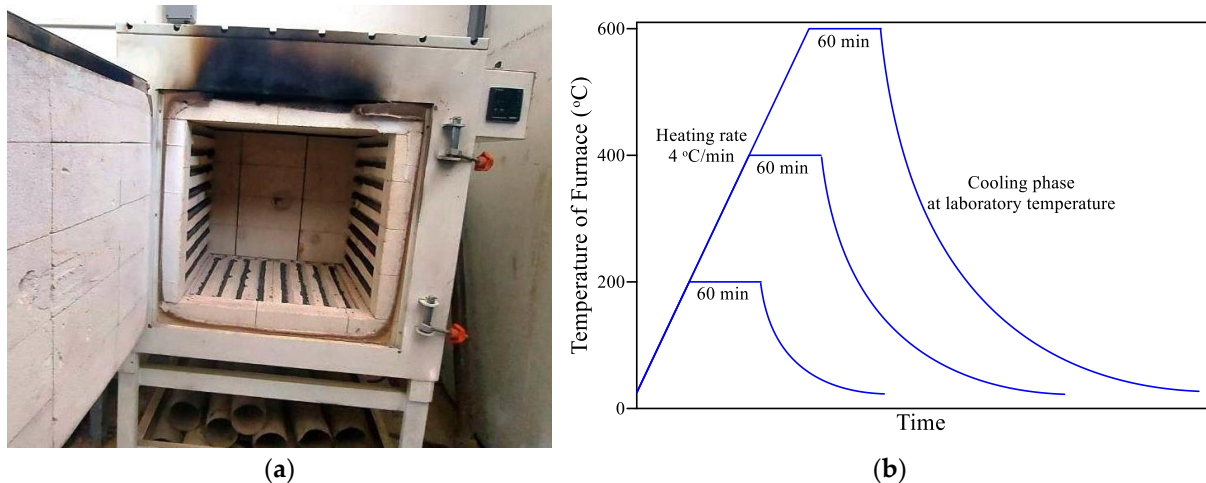


Figure 1. Heating of test specimens; (a) the electrical furnace; (b) the heating regime curve.

2.3. Repeated Drop-Weight Impact Test

The impact response of materials and structures can be experimentally evaluated using different types of tests, among which is the drop-weight one. ACI 544-2R [28] addressed two types of drop-weight tests. The first is the instrumented drop-weight test which is the most commonly used technique to evaluate the impact response of structural members. This test is mostly used for reinforced beam and slab elements and requires expensive sensor instrumentation and data acquisition equipment. On the other hand, the alternative drop-weight impact test is a very simple one that is conducted on small size specimens and requires no instrumentation or any sophisticated measurement systems. This test requires that a drop weight of 4.54 kg is dropped repeatedly on the test specimen from a height of 457 mm until a surface crack becomes visible, then the repeated impacts are resumed until the fracture failure of the specimen. The numbers of the impacts at which the first crack and failure occur are recorded as the cracking impact number and failure impact number. The test is generally considered as a qualitative evaluation technique, which compares the impact resistance of different concrete mixtures based on their ability to absorb higher or lower cracking and failure impact numbers.

The standard test specimen is a cylindrical (disk) with a diameter of approximately 150 mm and a thickness of approximately 64 mm. The standard test is operated manually by hand-lifting the drop weight to the specified drop height and releasing it to be freely dropped by gravity on a steel ball, which rests on the center of the specimen's top surface. The steel ball is used as a load distribution point and is held in place using a special framing system that also holds the concrete disk specimen, as illustrated in Figure 2a. However, it was found in previous works [27,32] that the manual operation requires significant effort and is time consuming, especially because at least 6 replication specimens are required to assess the test records due to the high dispersion of this test's results [27]. Therefore, an automatic repeated loading machine was manufactured to apply the standard dropping weight from the standard dropping height with a better accuracy and much less effort. The manufactured machine was provided with a high accuracy digital camera to observe the surface cracking and failure in addition to a special isolation cabin to reduce the test noise. The manufactured repeated drop weight impact testing machine is shown in Figure 2b.

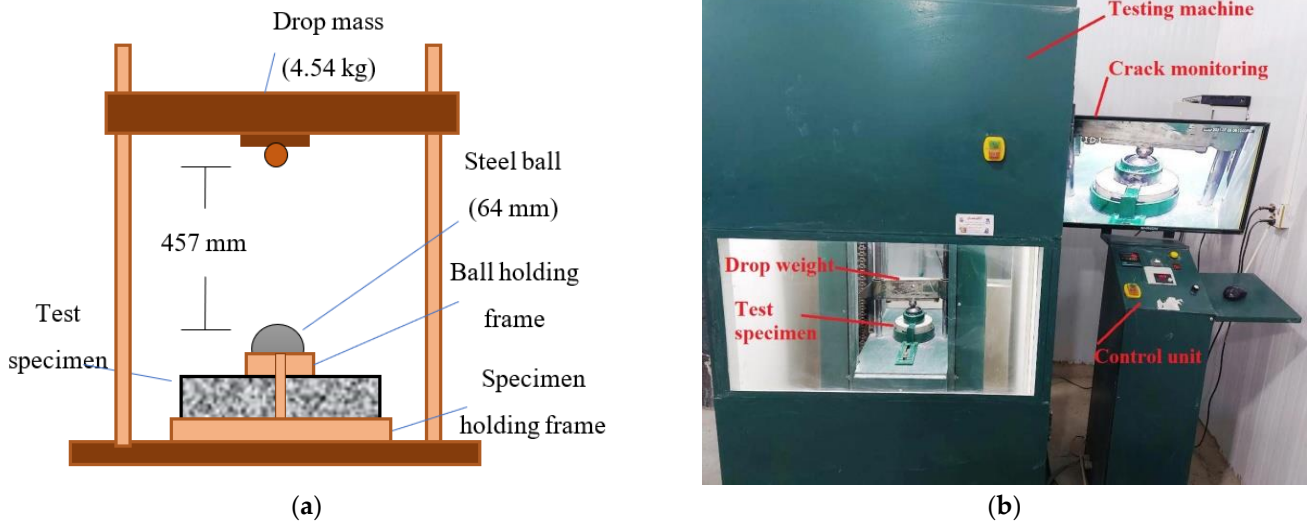


Figure 2. The drop-weight impact test; (a) schematic diagram of the test setup; (b) the automatic testing machine.

3. Results of Control Tests

3.1. Compressive Strength

The residual compressive strength–temperature relationship of the ECC tested cubes is shown in Figure 3, while Figure 4 shows that of the NC. It is clear in Figure 3 that the ECC strength reduced after exposure to 200 °C by approximately 22% compared to the reference unheated specimens, where the reference strength was 57.5 MPa, while it was 44.8 MPa after heating to 200 °C. A further decrease was recorded when the heating temperature was increased to 400 °C. However, this additional decrease was small compared to the initial one, where the residual strength percentages after exposure to 200 °C and 400 °C were approximately 78% and 70%, respectively. When the specimens were heated to 600 °C, a significant strength degradation was noticed with a residual compressive strength of 29.5 MPa, which means that the strength loss was approximately 49% compared to the strength of the unheated specimens. On the other hand, the percentage strength reduction of NC was less than that of the ECC after exposure to 200 °C and 400 °C. The residual compressive strength of the NC cubes after exposure to 200 °C and 400 °C was approximately 81% at both temperatures compared to the reference cubes as shown in Figure 4. However, the percentage residual compressive strength of the NC at 600 °C was approximately 50%, which was almost equal to that of the ECC (51.4%).

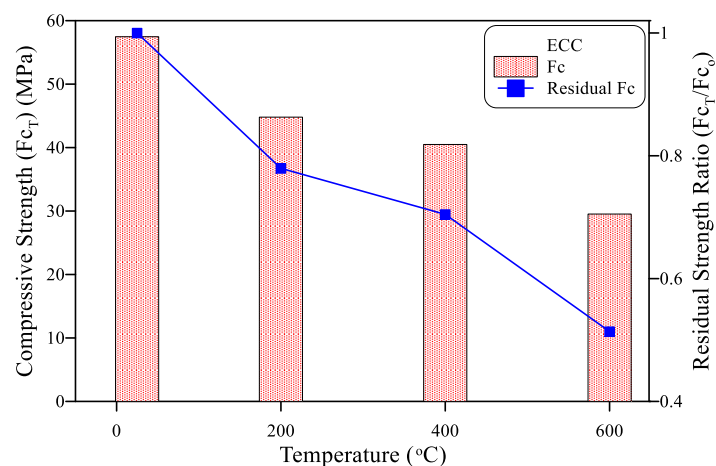


Figure 3. Residual compressive strength of ECC at different temperatures.

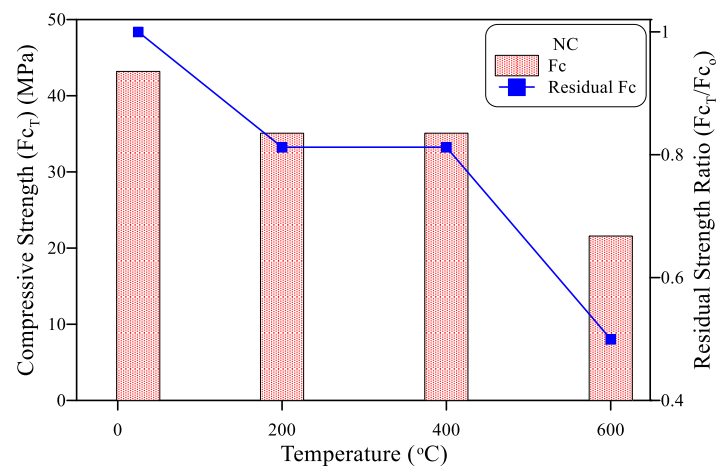


Figure 4. Residual compressive strength of NC at different temperatures.

The denser microstructure of ECCs compared to NC is considered as the main cause of the further strength reduction between 200 °C and 400 °C. ECCs comprise a much larger amount of very fine binder, fine silica sand, no coarse aggregate and lower water/cementitious material content, which in turn lowers the porosity of the ECC compared to the NC. The evaporation of the free pore water below 200 °C induces a pore pressure inside the microstructure. The dissipation of this pressure in the NC specimens due to the higher porosity relieves the internal thermal stresses, while these stresses are higher in the ECC due to the denser microstructure. As a result, the ECC suffered higher compressive strength losses at 200 °C and 400 °C. Previous researchers [53] reported that the total volume of the 0.1 micrometer and larger pores in the ECC reduced after exposure to 400 °C, which is attributed to the pozzolanic reaction of the unhydrated fly ash and other cementitious materials. Such a reaction would induce unfavorable volume changes due to the production of more C-S-H gel, which results in microstructural cracking leading to further strength degradation. The dehydration of hydrated products after exposure to temperatures higher than 400 °C is the main cause of the steep strength reduction at 600 °C, where this process leads to the degradation of the microstructure due to the increase of pore size and number and the further volume changes' micro-cracking. Sahmaran et al. [47] reported a significant increase in the volume and size of the pores of the ECC after exposure to 600 °C, where the porosity increased by 9% after exposure to 600 °C, which is large enough compared to 5% after exposure to 400 °C, while the pore size increased by at least 300% after 600 °C exposure.

3.2. Flexural Strength

As shown in Figure 5, the flexural strength of the ECC followed a continuous decrease behavior with temperature up to 600 °C. The reference flexural strength of the ECC at room temperature was 6.94 MPa, while it reduced to 5.75 MPa, 4.32 MPa and 2.31 MPa after exposure to 200 °C, 400 °C and 600 °C, respectively. This means that the strength respective reductions at these temperatures were approximately 17%, 38% and 67%. Similarly, the NC showed a continuous steep decrease in flexural strength with temperature increase as shown in Figure 6. The residual flexural strength records of the NC after heating to 200 °C, 400 °C and 600 °C were 2.87 MPa, 2.16 MPa and 0.32 MPa, while the reference unheated specimens recorded a flexural strength of 3.70 MPa. Hence, the percentage reductions were approximately 22%, 42% and 91% at 200 °C, 400 °C and 600 °C, respectively.

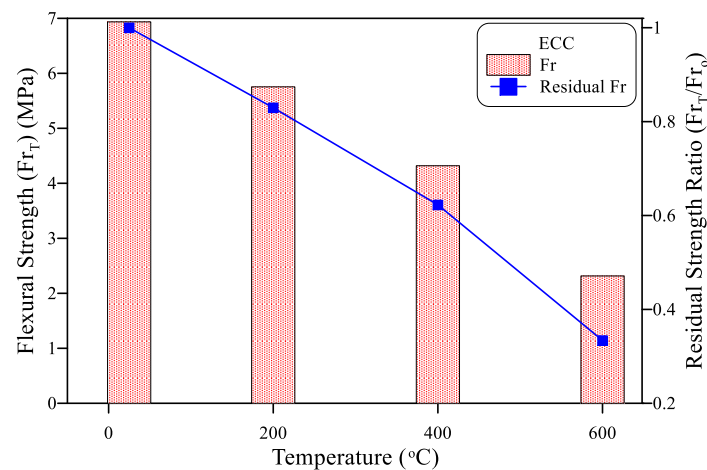


Figure 5. Residual flexural strength of ECC at different temperatures.

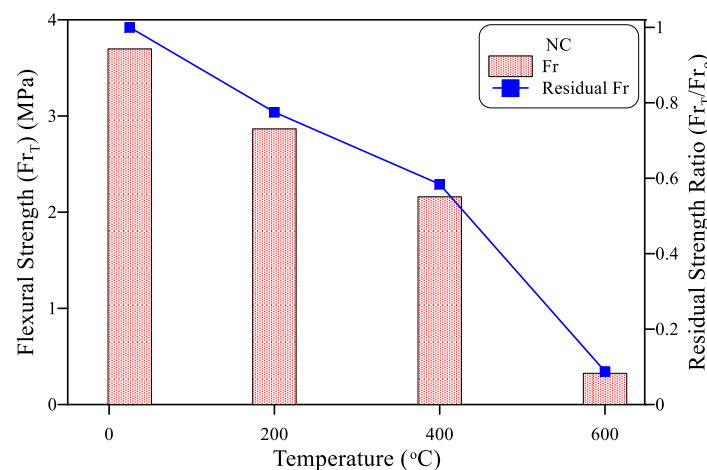


Figure 6. Residual flexural strength of NC at different temperatures.

The continuous decrease in the flexural strength after high temperature exposure is generally attributed to the volumetric changes in the cement matrix due to vapor movements beyond 100 °C and the bond loss between binder and filler after 400 °C due to their different thermal properties. In addition, most of the degradation at higher temperatures is attributed to the chemical reactions after 400 °C (dehydration of C-S-H) and the increased porosity as discussed in the previous section. As the flexural strength depends on the capability of concrete to withstand tensile stresses, the initial flexural strength was apparently higher for the ECC owing to the crack bridging activity of PP fibers, in addition to the higher content of cementitious materials. However, this bridging activity diminished after exposure to temperatures higher than 200 °C due to the melting of PP fibers. The better performance of the ECC at high temperatures compared to the NC might be attributed to the finer mixture constituents and the absence of coarse aggregate in the ECC, which minimized the effect of bond degradation. Wang et al. [54] showed that the residual flexural strength of PVA-based ECC after exposure to 400 °C was approximately 58% of the unheated strength, which is quite comparable to the obtained result in this study, while Yu et al. [55] reported that PVA-based ECC exhibited flexural strength reductions of more than 50% and more than 40% after exposure to temperatures of 400 °C and 600 °C, respectively.

4. Results of Repeated Impact Test

4.1. Description of Heated Specimens

Figure 7 shows the appearance of the external surfaces of a reference impact disk specimen and others heated to 200 °C, 400 °C and 600 °C before testing. No significant

changes in the specimens' appearance were noticed after high temperature exposure. However, it was observed that the gray color became lighter after 200 °C and small yellow areas were noticed on the surface of specimens exposed to 600 °C. This slight color change might be due to the decomposition of C-S-H gel particles [56–58]. It should also be noticed that PP fibers cannot sustain high temperatures where its melting point is less than 200 °C. As shown in Figure 8a, the presence of PP fibers had a significant impact in bridging the crack's opposite sides, resulting in a more gradual and ductile failure of the reference unheated specimens. On the other hand, the complete melting of fibers after exposure to 400 °C and higher eliminated this effect and created a more porous media. The channels left after fiber melting would connect and produce continuous porous networks, which have a positive effect by relieving the internal stresses due to the vapor pressure dissipation. On the other hand, these channels may have a negative effect by making the media more porous and hence more brittle under loads. Figure 8b shows that after exposure to 600 °C, the vaporization of PP fibers changed the internal color of the specimen to a dark gray and left a very porous structure behind.

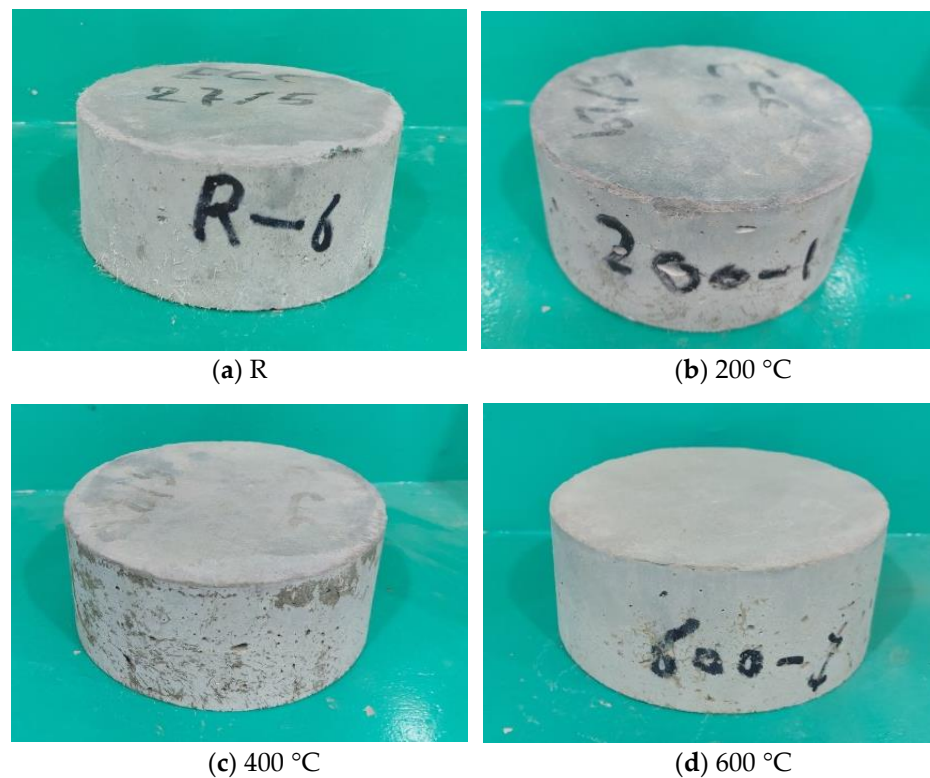


Figure 7. Impact test specimens subjected to different temperatures.



Figure 8. Physical appearance of PP fibers in the impact specimens before and after heating.

4.2. Cracking and Failure Impact Numbers

The recorded cracking numbers (Ncr) of the ECC and NC are shown in Figure 9 at different levels of high temperatures, while the results of failure numbers (Nf) are shown in Figure 10. It is worthy to mention that the ACI 542-2R test is known for the high dispersion of test results, where the Coefficient of Variation (COV) of the Ncr records of the ECC was in the range of 42% to 68.8%, while the COV of the recorded Nf results of the ECC specimens was in the range of 30.9% to 61.8%.

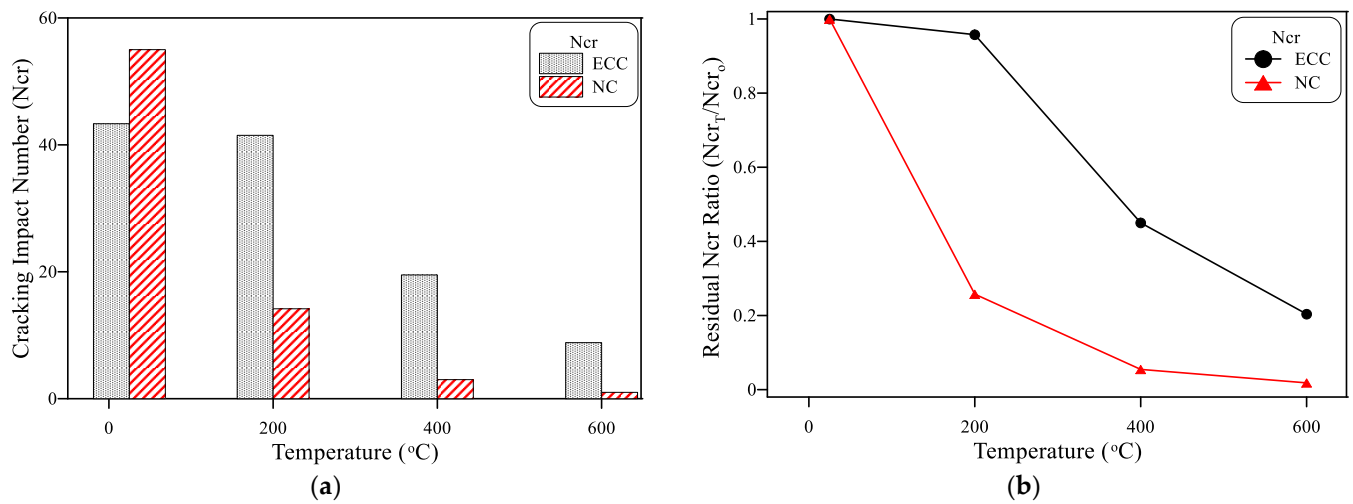


Figure 9. Residual cracking impact numbers of ECC and NC at different temperatures; (a) cracking number; (b) residual ratio of cracking number.

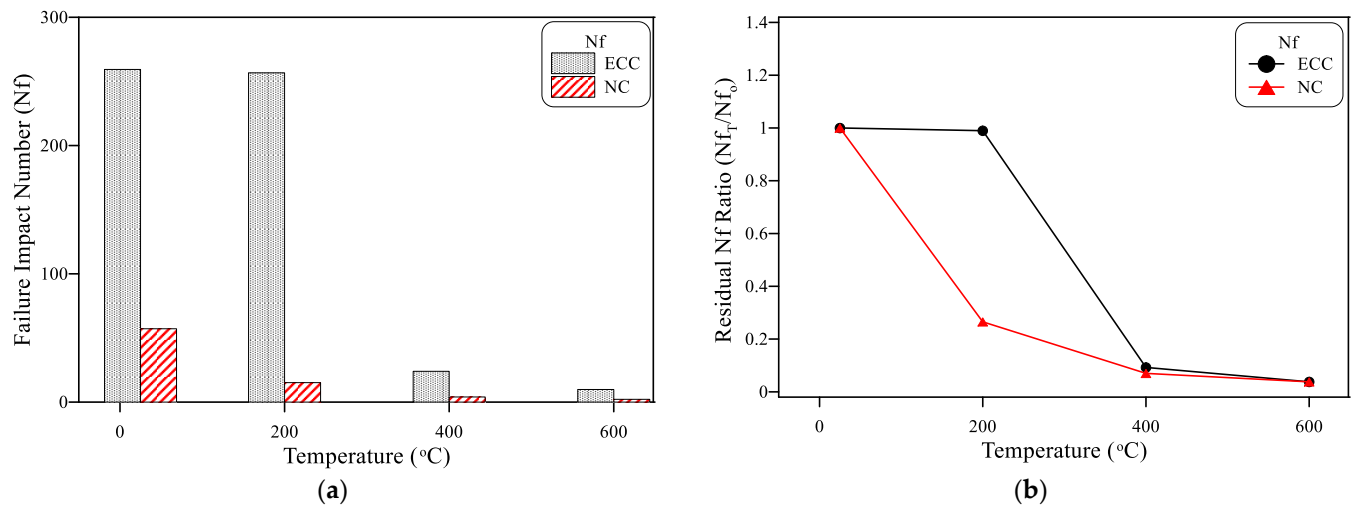


Figure 10. Residual failure impact numbers of ECC and NC at different temperatures; (a) failure number; (b) residual ratio of failure number.

Figure 9 shows that the reference unheated cracking number of the NC was higher than that of the ECC, which is attributed to the presence of gravel in the NC that enabled it to absorb a higher initial number of impacts before cracking. However, after high temperature exposure, the NC specimens showed much weaker response and deteriorated at much higher rate compared to the corresponding ECC specimens as shown in Figure 9a,b. The unheated Ncr of the ECC and NC were 43.3 and 55, respectively, noting that each impact number represents the average of six specimen records. On the other hand, the residual ECC cracking numbers were 41.5, 19.5 and 8.8 after exposure to 200 °C, 400 °C and 600 °C, respectively, while those of the NC specimens were 14.2, 3 and 1, respectively.

The results reveal a steep drop in the cracking impact numbers of the NC, where the percentage residual Ncr values were only 25.8%, 5.5% and 1.8%, respectively, compared to the reference unheated number as shown in Figure 9b. On the other hand, the ECC showed an insignificant decrease (less than 5%) after exposure to 200 °C, while the percentage residual Ncr values were 45% and 20.4% after exposure to 400 °C and 600 °C, respectively. The rapid decrease of the Ncr of the NC is attributed to the discussed physical and chemical changes that occur after exposure to high temperatures, especially the dehydration of C-S-H, which deteriorates the cement matrix, in addition to the different thermal movements of cement paste and aggregate. Consequently, the internal structure becomes more and more brittle as the temperature increases, which leads to the loss of impact energy absorption capacity and hence to rapid cracking. On the other hand, the higher cementitious materials content, the finer matrix and the absence of aggregate reduced these effects and enabled the ECC specimen to continue withstanding more impacts before cracking. It should be noticed that although the melting point of PP fibers is less than 200 °C, a significant amount of these fibers still existed in the specimens heated to 200 °C. These fibers helped maintain a significant impact number before cracking, which is approximately equal to that of the unheated specimens (95.8%). Aslani et al. [59] reported that PVA fibers did not melt completely after exposure to 300 °C, which is higher than the approximate melting point of PVA (200 °C to 230 °C).

ECCs are known for their high ability to withstand plastic deformation after cracking under tensile and flexural loads, which is attributed to their unique microstructure with high content of binder and fine filler in addition to the potential of fibers to withstand high tensile stresses across the cracks. These characteristics enabled the ECC specimens to absorb significantly higher energy compared to NC after cracking. The test results of this study showed that this potential is also valid under repeated impact loads. As shown in Figure 10, the failure impact number (Nf) of the unheated ECC specimens jumped to a very high limit compared to its corresponding Ncr, while that of NC was comparable to its cracking number, which duplicated the difference of Nf between the ECC and NC several times although the Ncr of the NC was higher than that of the ECC. The Nf of the unheated ECC was 259.3, while that of the NC was only 57.2. This means that the Nf of the NC was approximately equal to its Ncr with only 2.2 higher impacts, while the ECC sustained 216 more impacts after cracking.

After exposure to 200 °C, the NC specimens lost approximately 73% of their initial failure impact performance and retained only 15.2 impacts at failure. Oppositely, the ECC specimens kept approximately the same failure strength of the unheated specimens due to the same reasons discussed above. As shown in Figure 10b, the residual Nf of the ECC after exposure to 200 °C was 99% of the corresponding unheated Nf with 256.7 impacts. As discussed previously, the PP fibers did not melt completely at 200 °C, which means that the fiber bridging activity was still partially effective after cracking. The hydration of the unhydrated products at this temperature might be another reason that enabled the specimens to sustain high impact numbers before cracking. On the other hand, as temperature increased beyond 200 °C, the microstructure of the ECC deteriorated steeply after the complete melting and vaporization of the PP fibers (around 340 °C [60]) and the decomposition of C-S-H gel, which resulted in a weak microstructure. Therefore, the impact strength deteriorated sharply after exposure to 400 °C and 600 °C. As shown in Figure 10b, the percentage residuals of the Nf after exposure to these temperatures were only 9.2% and 3.8%, respectively.

4.3. Failure Patterns of Impact Specimens

The post-failure appearance of a reference ECC specimen and others heated to different high temperatures after repeated impact loading are shown in Figure 11. It is clear in Figure 11a that the central loading area of the top surface of the reference specimen was fractured due to the damage. This fracture zone occurred under the effect of the repeated concentrated compressive stresses from the steel ball, which reflects the ability of the

material to absorb significant impact energy under the concentrated impact loading. After the fracture of the surface layer, the PP fibers kept bridging the internal micro-cracks where the compressive impacts try to split the cylinder and hence induce internal tensile stresses, see Figure 8a. However, the continuous impacting could finally break the fibers or their bond with the surrounding media resulting in a progressive crack widening and propagation. Hence, the surface cracks become visible. As shown in Figure 11a, the reference specimens exhibited a ductile failure behavior with central fracture zone and multi-surface cracking.

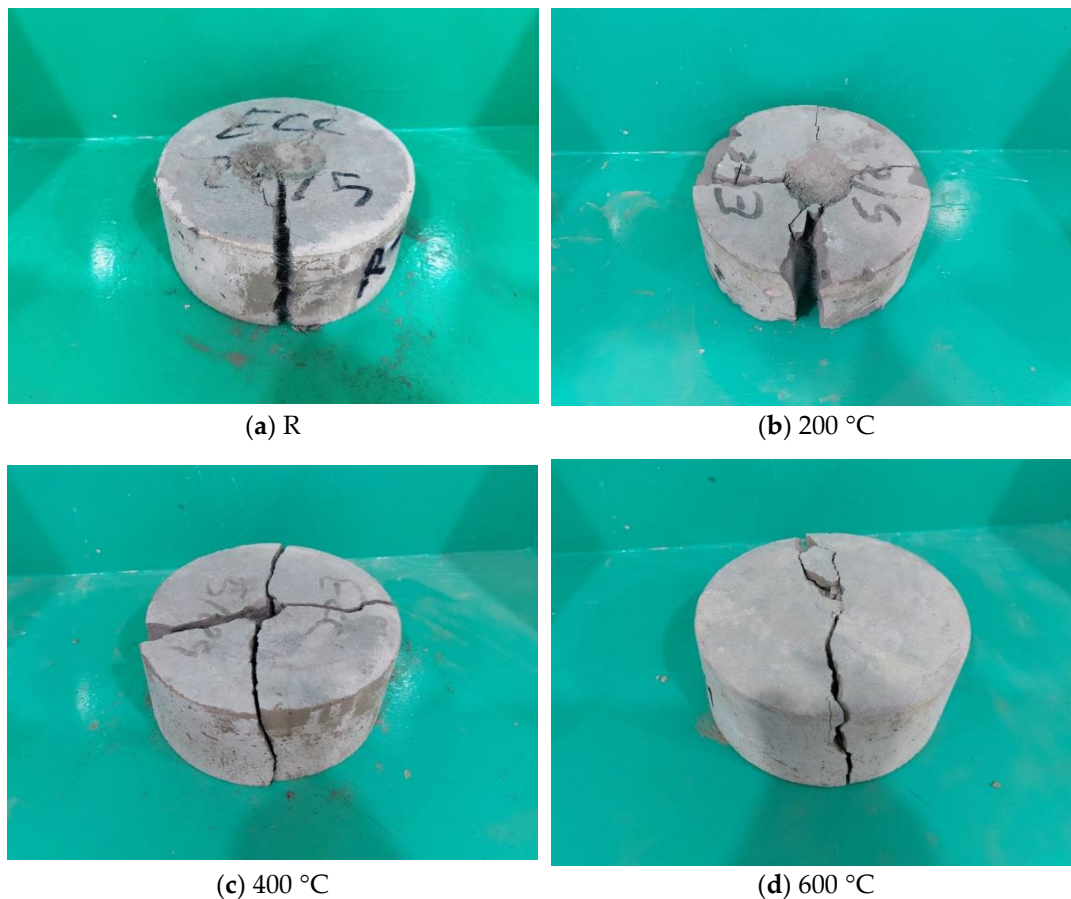


Figure 11. Failure patterns of tested impact specimens heated to different temperatures.

Referring to the impact response of the ECC specimens after exposure to 200 °C, the failure pattern at this temperature was similar to that of the reference unheated specimens, but with a lower number of standing fibers across the mouth of the main crack. It should also be noticed that the other minor cracks were wider at this temperature (Figure 11b) compared to those of the specimens, which discloses the lower ductility and higher brittleness of the heated specimens. As previously disclosed, the heating to 400 °C and 600 °C caused serious damage to the microstructure of the ECC and vaporized the reinforcing elements (PP fibers), which was approved by the brittle and sudden failure of the specimens to two, three or four pieces with wide cracks. This failure was not associated with central fracturing as in the case of the reference and 200 °C specimens, where the thermally weakened structure could not absorb significant concentrated impacts, as shown in Figure 11c,d.

5. Strength Correlation with Temperature

In some cases, it is required to evaluate the residual strength of a material after exposure to a specific temperature. If sufficient experimental data are not available, extrapolation from other existing data may be considered satisfactory for a quick primary evaluation.

Despite the limited number of points for each fit, simplified correlations were introduced, as shown in Figure 12, to describe the relation of the strength and impact numbers of the PP-based ECC after exposure to high temperatures. Figure 12a shows that the relations of both compressive strength and flexural strength with temperature can be represented using linear fits with good determination coefficients (R^2) of 0.96 and 0.99, respectively. Referring to Figure 12c, it can be said that a multilinear relation would better describe the reduction of compressive strength with temperature. However, a determination coefficient of 0.96 is good enough to accept the simpler linear correlation.

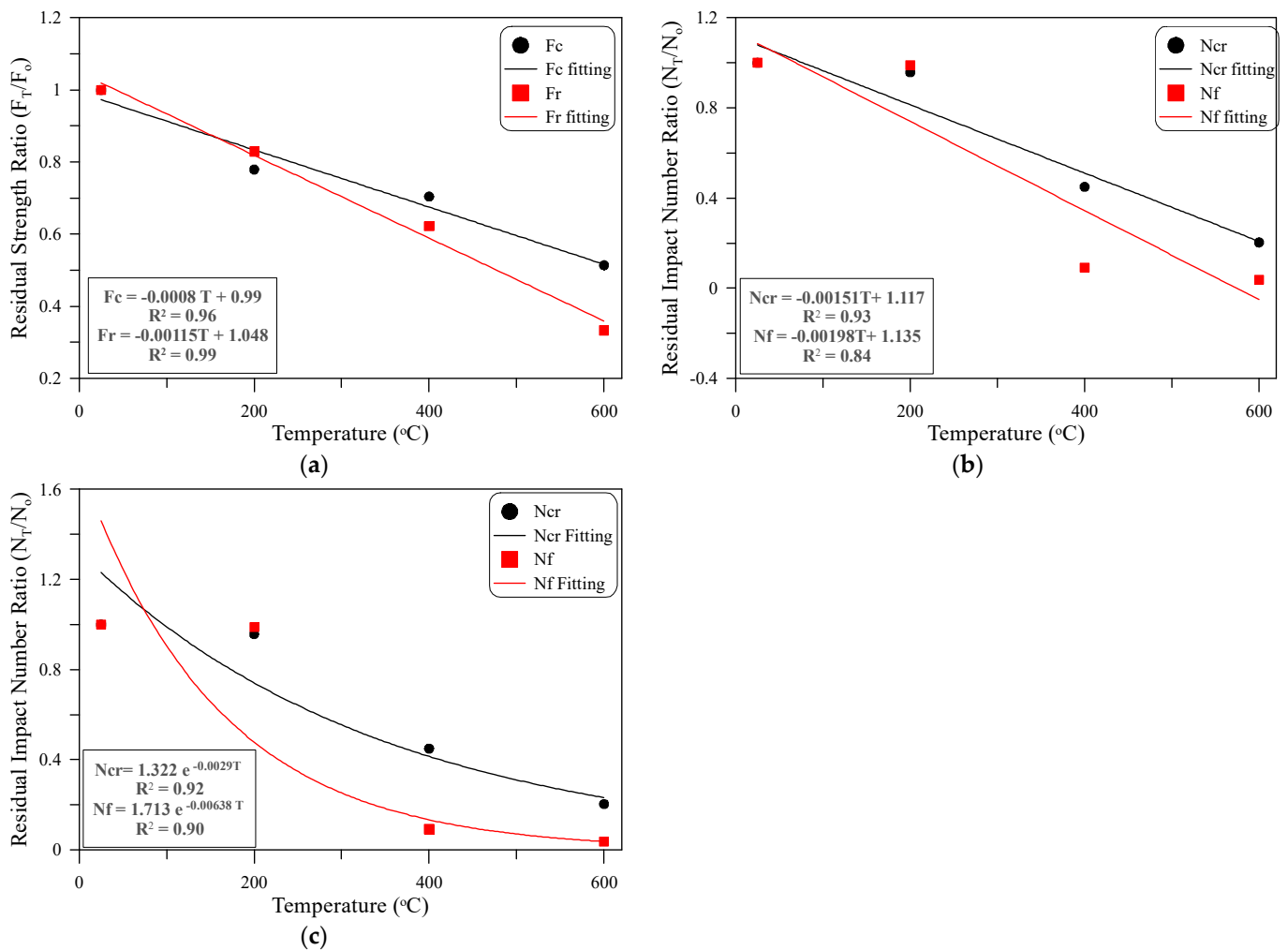


Figure 12. Correlation with temperature; (a) linear correlation of strength; (b) linear correlation of impact numbers; (c) exponential correlation of impact numbers.

The impact numbers showed a weaker linear correlation degree with temperature than those of compressive strength and flexural strength. As shown in Figure 12b, the linear relations of N_{cr} and N_f with temperature underestimate the retained impact numbers at 200 $^{\circ}C$, while that of N_f overestimates the experimental failure impact number recorded at 400 $^{\circ}C$. The deviations from the experimental records at these temperatures impacted the degree of the linear correlation, especially for N_f , where the R^2 of the linear correlation was 0.84, which is the lowest among the obtained ones. To avoid such a low degree of correlation, nonlinear correlations were tried and the exponential one was found to give a coefficient of determination of 0.9, which is quite acceptable as an indication of a good correlation. As shown in Figure 12c, the exponential correlations could acceptably estimate the degradation of N_{cr} and N_f after exposure to the highest temperatures (400 $^{\circ}C$ and

600 °C). However, these correlations significantly underestimated the residual impact numbers after exposure to 200 °C.

6. Conclusions

Compressive, flexural and repeated impact tests were conducted in this study to evaluate the residual strength of PP fiber-based ECCs after exposure to high temperatures up to 600 °C. Based on the results obtained from the experimental work of this study, the following are the most important conclusions:

1-The compressive strength of the ECC decreased with temperature increase. However, the residual strength at 400 °C was close to that at 200 °C, while exposure to 600 °C led to a significant strength reduction. The percentage residual compressive strengths of the tested ECC cubes after exposure to 200 °C, 400 °C and 600 °C were approximately 78%, 70% and 51%, respectively. The reason for the strength deterioration after 400 °C is attributed to the chemical and physical changes within the material microstructure due to the temperature exposure, which include the decomposition of C-S-H gel and the increase of porosity owing to the vaporization of PP fibers. The linear correlation could effectively describe the degradation of compressive strength after high temperature exposure with an R^2 of 0.96.

2-The flexural strength of the ECC showed a clear continuous reduction with temperature compared to that of compressive strength and higher percentage reductions at 400 °C and 600 °C. Therefore, the linear correlation with temperature was the most accurate one among the conducted tests with an R^2 of 0.99. The residual flexural strengths were reduced to approximately 62 and 33% after heating to 400 °C and 600 °C, respectively.

3-The ECC specimens exhibited minor reductions in the cracking number (Ncr) after exposure to 200 °C with a residual percentage of approximately 96%. The reduction in Ncr was much higher after exposure to the higher temperatures. However, the deterioration of normal concrete (NC) was much faster. ECCs retained percentage residual Ncr values of approximately 45% and 20% after exposure to 400 °C and 600 °C, respectively, while the corresponding percentages of NC were approximately 5% and 2%. The much higher binder content, finer matrix and the absence of aggregate enabled the heated ECC specimen to continue absorbing higher impacts till cracking compared to NC.

4-The failure impact number of the unheated ECC specimens jumped several times higher than the corresponding Ncr, which assured the ability of the dense and fine microstructure of the ECCs, with the help of the PP-fibers crack bridging elements, to amplify the capacity impact energy absorption at failure. The retained Nf was 259.3, which was approximately 4.5 times that of NC although of the higher Ncr of NC. After exposure to 200 °C, the ECC retained almost the same unheated Nf number (99%), while NC retained only 27% of its unheated failure number. Oppositely, both ECC and NC sharply lost their impact resistances after exposure to 400 °C and 600 °C with percentage residual Nf values of less than 10%, and 4%, respectively.

5-The linear correlation was found suitable to describe the reduction of Ncr with temperature with a good R^2 of 0.93. However, such correlation noticeably underestimated the recorded Nf at 200 °C and overestimated that at 400 °C, which decreased its R^2 to 0.84. On the other hand, the exponential relation was found to better describe the deterioration of Nf after high temperature exposure, where R^2 was 0.9.

Author Contributions: Conceptualization, S.R.A.; methodology, R.A.A.-A. and S.R.A.; validation, S.R.A. and M.Ö.; formal analysis, S.R.A. and R.A.A.-A.; resources, R.A.A.-A.; data curation, S.R.A. and R.A.A.-A.; writing—original draft preparation, S.R.A. and R.A.A.-A.; writing—review and editing, S.R.A. and M.Ö.; visualization, S.R.A. and R.A.A.-A.; supervision, S.R.A. and M.Ö.; project administration, S.R.A. and M.Ö. All authors have read and agreed to the published version of the manuscript.

Funding: This research received no external funding.

Institutional Review Board Statement: Not Applicable.

Informed Consent Statement: Not Applicable.

Data Availability Statement: Data are available upon request from the corresponding author.

Acknowledgments: The authors acknowledge the support from Al-Sharq Lab., Kut, Wasit, Iraq and Ahmad A. Abbas.

Conflicts of Interest: The authors declare no conflict of interest.

References

1. Arna'ot, F.H.; Abid, S.R.; Özakça, M.; Tayşi, N. Review of concrete flat plate-column assemblies under fire conditions. *Fire Saf. J.* **2017**, *93*, 39–52. [[CrossRef](#)]
2. Brushlinsky, N.N.; Ahrens, M.; Sokolov, S.V.; Wagner, P. World fire statistics, Center of Fire Statistics of CTIF. *Int. Assoc. Fire Rescue Serv.* **2018**, *21*, 11.
3. Albrektsson, J.; Flansbjerg, M.; Lindqvist, J.E.; Jansson, R. *Assessment of Concrete Structures after Fire*; SP Report 19; SP Technical Research Institute of Sweden: Boras, Sweden, 2011; p. 93.
4. Guo, Y.; Zhang, J.; Chen, G.; Xie, Z. Compressive behaviour of concrete structures incorporating recycled concrete aggregates, rubber crumb and reinforced with steel fibre, subjected to elevated temperatures. *J. Clean. Prod.* **2014**, *72*, 193–203. [[CrossRef](#)]
5. Tufail, M.; Shahzada, K.; Gencturk, B.; Wei, J. Effect of elevated temperature on mechanical properties of limestone, quartzite and granite concrete. *Int. J. Concr. Struct. Mater.* **2017**, *11*, 17–28. [[CrossRef](#)]
6. Babalola, O.E.; Awoyera, P.O.; Le, D.-H.; Bendezú Romero, L.M. A review of residual strength properties of normal and high strength concrete exposed to elevated temperatures: Impact of materials modification on behaviour of concrete composite. *Constr. Build. Mater.* **2021**, *296*, 123448. [[CrossRef](#)]
7. Roufael, G.; Beaucour, A.-L.; Eslami, J.; Hoxha, D.; Noumowe, A. Influence of lightweight aggregates on the physical and mechanical residual properties of concrete subjected to high temperatures. *Constr. Build. Mater.* **2021**, *268*, 121221. [[CrossRef](#)]
8. Drzymala, T.; Jackiewicz-Rek, W.; Tomaszewski, M.; Kus, A.; Galaj, J.; Sukys, R. Effects of high temperatures on the properties of high performance concrete (HPC). *Procedia Eng.* **2017**, *172*, 256–263. [[CrossRef](#)]
9. Abrams, M.S. *Compressive Strength of Concrete at Temperatures to 1600 °F. ACI SP 25, Temperature and Concrete*; American Concrete Institute ACI: Detroit, MI, USA, 1971.
10. Dügenci, O.; Haktanir, T. Experimental research for the effect of high temperature on the mechanical properties of steel fiber-reinforced concrete. *Constr. Build. Mater.* **2015**, *75*, 82–88. [[CrossRef](#)]
11. Arna'ot, F.H.; Abbass, A.A.; Abualtemen, A.A.; Abid, S.R.; Özakça, M. Residual strength of high strength concentric column-SFRC flat plate exposed to high temperatures. *Constr. Build. Mater.* **2017**, *154*, 204–218. [[CrossRef](#)]
12. Chu, H.-Y.; Jiang, J.-Y.; Sun, W.; Zhang, M. Mechanical and physicochemical properties of ferro-siliceous concrete subjected to elevated temperatures. *Constr. Build. Mater.* **2016**, *122*, 743–752. [[CrossRef](#)]
13. Phan, L.T.; Carino, N.J. Code provisions for high strength concrete strength-temperature relationship at elevated temperatures. *Mater. Struct.* **2003**, *36*, 91–98. [[CrossRef](#)]
14. Netinger, I.; Kesegic, I.; Guljas, I. The effect of high temperatures on the mechanical properties of concrete made with different types of aggregates. *Fire Saf. J.* **2011**, *46*, 425–430. [[CrossRef](#)]
15. Deng, Z.H.; Huang, H.Q.; Ye, B.; Wang, H.; Xiang, P. Investigation on recycled aggregate concretes exposed to high temperature by biaxial compressive tests. *Constr. Build. Mater.* **2020**, *244*, 118048. [[CrossRef](#)]
16. Phan, L.T.; Carino, N.J. Review of mechanical properties of HSC at elevated temperatures. *J. Mater. Civ. Eng.* **1998**, *10*, 58–64. [[CrossRef](#)]
17. Al-Owaisy, S.R. Effect of high temperatures on shear transfer strength of concrete. *J. Eng. Sustain. Dev.* **2007**, *11*, 92–103.
18. Sultan, H.K.; Alyaseri, I. Effects of elevated temperatures on mechanical properties of reactive powder concrete elements. *Constr. Build. Mater.* **2020**, *261*, 120555. [[CrossRef](#)]
19. Cheng, F.P.; Kodur, V.K.R.; Wang, T.C. Stress-strain curves for high strength concrete at elevated temperatures. *J. Mater. Civ. Eng.* **2004**, *16*, 84–94. [[CrossRef](#)]
20. Husem, M. The effects of high temperature on compressive and flexural strengths of ordinary and high-performance concrete. *Fire Saf. J.* **2006**, *41*, 155–163. [[CrossRef](#)]
21. Al-Owaisy, S.R. Strength and elasticity of steel fiber reinforced concrete at high temperatures. *J. Eng. Sustain. Dev.* **2007**, *11*, 125–133.
22. Toric, N.; Boko, I.; Peroš, B. Reduction of postfire properties of high-strength concrete. *Adv. Civ. Eng.* **2013**, *2013*, 712953.
23. Alimrani, N.; Balazs, G.L. Investigations of direct shear of one-year old SFRC after exposed to elevated temperatures. *Constr. Build. Mater.* **2020**, *254*, 119308. [[CrossRef](#)]
24. Nili, M.; Afroughsabet, V. Combined effect of silica fume and steel fibers on the impact resistance and mechanical properties of concrete. *Int. J. Impact Eng.* **2010**, *37*, 879–886. [[CrossRef](#)]
25. Salaimanimagudam, M.P.; Suribabu, C.R.; Murali, G.; Abid, S.R. Impact response of hammerhead pier fibrous concrete beams designed with topology optimization. *Period. Polytech. Civ. Eng.* **2020**, *64*, 1244–1258. [[CrossRef](#)]
26. Wang, W.; Chouw, N. The behavior of coconut fibre reinforced concrete (CFRC) under impact loading. *Constr. Build. Mater.* **2017**, *134*, 452–461. [[CrossRef](#)]

27. Abid, S.R.; Abdul-Hussein, M.L.; Ali, S.H.; Kazem, A.F. Suggested modified testing techniques to the ACI 544-R repeated drop-weight impact test. *Constr. Build. Mater.* **2020**, *244*, 118321. [[CrossRef](#)]
28. ACI 544-2R. *Measurement of Properties of Fiber Reinforced Concrete*; American Concrete Institute: Detroit, MI, USA, 1999.
29. Mastali, M.; Dalvand, A. The impact resistance and mechanical properties of self-compacting concrete reinforced with recycled CFRP pieces. *Compos. B Eng.* **2016**, *92*, 360–376. [[CrossRef](#)]
30. Ismail, M.K.; Hassan, A.A. Impact resistance and mechanical properties of self-consolidating rubberized concrete reinforced with steel fibers. *ASCE J. Mater. Civ. Eng.* **2017**, *29*, 04016193. [[CrossRef](#)]
31. Mahakavi, P.; Chithra, R. Impact resistance, microstructures and digital image processing on self-compacting concrete with hooked end and crimped steel fiber. *Constr. Build. Mater.* **2019**, *220*, 651–666. [[CrossRef](#)]
32. Jabir, H.A.; Abid, S.R.; Murali, G.; Ali, S.H.; Klyuev, S.; Fediuk, R.; Vatin, N.; Promakhov, V.; Vasilev, Y. Experimental Tests and Reliability Analysis of the Cracking Impact Resistance of UHPFRC. *Fibers* **2020**, *8*, 74. [[CrossRef](#)]
33. Abid, S.R.; Abdul-Hussein, M.L.; Ayoob, N.S.; Ali, S.H.; Kadhum, A.L. Repeated drop-weight impact tests on self-compacting concrete reinforced with micro-steel fiber. *Heliyon* **2020**, *6*, e03198. [[CrossRef](#)]
34. Abid, S.R.; Murali, G.; Ali, S.H.; Kadhum, A.L.; Al-Gasham, T.S.; Fediuk, R.; Vatin, N.; Karelina, M. Impact performance of steel fiber-reinforced self-compacting concrete against repeated drop weight impact. *Crystals* **2021**, *11*, 91. [[CrossRef](#)]
35. Abid, S.R.; Ali, S.H.; Goaz, H.A.; Al-Gasham, T.S.; Kadhum, A.L. Impact resistance of steel fiber-reinforced self-compacting concrete. *Mag. Civ. Eng.* **2021**, *105*, 10504.
36. Murali, G.; Abid, S.R.; Mugahed Amran, Y.H.; Abdelgader, H.S.; Fediuk, R.; Susrutha, A.; Poonguzhali, K. Impact performance of novel multi-layered prepacked aggregate fibrous composites under compression and bending. *Structures* **2020**, *28*, 1502–1515. [[CrossRef](#)]
37. Murali, G.; Abid, S.R.; Karthikeyan, K.; Haridharan, M.K.; Amran, M.; Siva, A. Low-velocity impact response of novel prepacked expanded clay aggregate fibrous concrete produced with carbon nano tube, glass fiber mesh and steel fiber. *Constr. Build. Mater.* **2021**, *284*, 122749. [[CrossRef](#)]
38. Murali, G.; Abid, S.R.; Abdelgader, H.S.; Amran, M.Y.H.; Shekarchi, M.; Wilde, K. Repeated projectile impact tests on multi-layered fibrous cementitious composites. *Int. J. Civ. Eng.* **2021**, *19*, 635–651. [[CrossRef](#)]
39. Murali, G.; Abid, S.R.; Amran, M.; Fediuk, R.; Vatin, N.; Karelina, M. Combined effect of multi-walled carbon nanotubes, steel fibre and glass fibre mesh on novel two-stage expanded clay aggregate concrete against impact loading. *Crystals* **2021**, *11*, 720. [[CrossRef](#)]
40. Murali, G.; Asrani, N.P.; Ramkumar, V.R.; Siva, A.; Haridharan, M.K. Impact Resistance and Strength Reliability of Novel Two-Stage Fibre-Reinforced Concrete. *Arab. J. Sci. Eng.* **2019**, *44*, 4477–4490. [[CrossRef](#)]
41. Ramkumar, V.R.; Murali, G.; Asrani, N.P.; Karthikeyan, K. Development of a novel low carbon cementitious two stage layered fibrous concrete with superior impact strength. *J. Build. Eng.* **2019**, *25*, 100841. [[CrossRef](#)]
42. Prasad, N.; Murali, G. Exploring the impact performance of functionally-graded preplaced aggregate concrete incorporating steel and polypropylene fibres. *J. Build. Eng.* **2021**, *35*, 102077. [[CrossRef](#)]
43. Ramakrishnan, K.; Depak, S.; Hariharan, K.; Abid, S.R.; Murali, G.; Cecchin, D.; Fediuk, R.; Amran, Y.M.; Abdelgader, H.S.; Khatib, J.M. Standard and modified falling mass impact tests on preplaced aggregate fibrous concrete and slurry infiltrated fibrous concrete. *Constr. Build. Mater.* **2021**, *298*, 123857. [[CrossRef](#)]
44. Li, V.C. From micromechanics to structural engineering: The design of cementitious composites for civil engineering applications. *J. Struct. Mech. Earthq. Eng.* **1993**, *10*, 37–48. [[CrossRef](#)]
45. Li, V.C. *Engineering Cementitious Composites (ECC)-Materials, Structural, and Durability Performance*; University of Michigan: Ann Arbor, MI, USA, 2007.
46. Ismail, M.K.; Hassan, A.A.A.; Lachemi, M. Performance of self-consolidating engineered cementitious composite under drop-weight impact loading. *ASCE J. Mater. Civ. Eng.* **2019**, *31*, 04018400. [[CrossRef](#)]
47. Sahmaran, M.; Lachemi, M.; Li, V. Assessing mechanical properties and microstructure of fire-damaged engineered cementitious composites. *ACI Mater. J.* **2010**, *107*, 297–304.
48. Çavdar, A. A study on the effects of high temperature on mechanical properties of fiber reinforced cementitious composites. *Compos. B* **2012**, *43*, 2452–2463. [[CrossRef](#)]
49. Shang, X.; Lu, Z. Impact of high temperature on the compressive strength of ECC. *Adv. Mater. Sci. Eng.* **2014**, *2014*, 919078. [[CrossRef](#)]
50. Raffei, P.; Shokravi, H.; Mohammadyan-Yasouj, S.E.; Kolor, S.S.R.; Petru, M. Temperature impact on engineered cementitious composite containing basalt fibers. *Appl. Sci.* **2021**, *11*, 6848. [[CrossRef](#)]
51. BS EN 12390-3: 2009; Testing Hardened Concrete-Part 3: Compressive Strength of Test Specimens. British Standards: London, UK, 2009.
52. BS EN 12390-5: 2009; Testing Hardened Concrete-Part 5: Flexural Strength of Test Specimens. British Standards: London, UK, 2009.
53. Şahmaran, M.; Özbay, E.; Yücel, H.E.; Lachemi, M.; Li, V.C. Effect of fly ash and PVA fiber on microstructural damage and residual properties of engineered cementitious composites exposed to high temperatures. *J. Mater. Civ. Eng.* **2011**, *23*, 1735–1745. [[CrossRef](#)]

54. Wang, Z.-B.; Han, S.; Sun, P.; Liu, W.-K.; Wang, Q. Mechanical properties of polyvinyl alcohol-basalt hybrid fiber engineered cementitious composites with impact of elevated temperatures. *J. Cent. South Univ.* **2021**, *28*, 1459–1475. [[CrossRef](#)]
55. Yu, Z.; Yuan, Z.; Xia, C.; Zhang, C. High temperature flexural deformation properties of engineered cementitious composites (ECC) with hybrid fiber reinforcement. *Res. Appl. Mater. Sci.* **2020**, *2*, 17–26. [[CrossRef](#)]
56. Li, Q.-H.; Sun, C.-J.; Xu, S.-L. Thermal and mechanical properties of ultrahigh toughness cementitious composite with hybrid PVA and steel fibers at elevated temperatures. *Compos. B* **2019**, *176*, 107201. [[CrossRef](#)]
57. Li, Q.; Gao, X.; Xu, S.; Peng, Y.; Fu, Y. Microstructure and mechanical properties of high-toughness fiber-reinforced cementitious composites after exposure to elevated temperatures. *J. Mater. Civ. Eng.* **2016**, *28*, 04016132. [[CrossRef](#)]
58. Liu, J.-C.; Tan, K.H.; Fan, S.-X. Residual mechanical properties and spalling resistance of strain-hardening cementitious composite with Class C fly ash. *Constr. Build. Mater.* **2017**, *181*, 253–265. [[CrossRef](#)]
59. Aslani, F.; Wang, L. Fabrication and characterization of an engineered cementitious composite with enhanced fire resistance performance. *J. Clean. Prod.* **2019**, *221*, 202–214. [[CrossRef](#)]
60. Poon, C.S.; Shui, Z.H.; Lam, L. Compressive behavior of fiber reinforced high-performance concrete subjected to elevated temperatures. *Cem. Concr. Res.* **2004**, *34*, 2215–2222. [[CrossRef](#)]